The role of the spin polarization in x-ray magnetic circular dichroism spectra of itinerant magnets

1997 J. Phys.: Condens. Matter 9 L259

(http://iopscience.iop.org/0953-8984/9/18/002)

J. Phys.: Condens. Matter **9** (1997) L259–L265. Printed in the UK PII: S0953-8984(97)81266-0

LETTER TO THE EDITOR

The role of the spin polarization in x-ray magnetic circular dichroism spectra of itinerant magnets

Gerrit van der Laan†

Daresbury Laboratory, Warrington WA4 4AD, UK

Received 20 February 1997

Abstract. The spectral shape of the 2p x-ray magnetic circular dichroism (XMCD) in 3d metallic magnets is shown to change systematically as a function of spin polarization. Using an independent-particle model we can obtain the line shape by adding up the individual contributions from each of the ground-state moments. It is found that the charge distribution and the magnetism have completely different influences on the spectral shape.

The physics of magnetic phenomena such as perpendicular magnetic anisotropy, giant magnetoresistance and oscillatory exchange coupling in thin films and multilayers composed of different magnetic materials is currently under intense investigation. This is strongly motivated by technological applications in magneto-optical recording devices and magnetic sensors. Furthermore, recent experimental and theoretical advances in x-ray magnetic circular dichroism (XMCD) have made it possible to separate the spin and orbital contributions to the magnetic moments of each element in a composite material. Theoretical sum rules relate the integrated difference signal in absorption between left and right circularly polarized x-rays at the 2p absorption edges to ground-state magnetic moments of 3d transition metals [1–4]. However, the information contained in the detailed structure of these spectra has been largely ignored so far although recent measurements across the 3d transition-metal series show large changes in the line shape [5, 6].

In a lucid picture the 2p XMCD process can be visualized by a two-step model [7]. The core level is split into $j = \frac{3}{2}$ and $\frac{1}{2}$ states where spin and orbit are coupled parallel and antiparallel, respectively. In the first step the emission with the light helicity vector parallel (antiparallel) to the 2p orbital moment results in photoelectrons of preferred spin up (down) direction. In the second step these photoelectrons have to find their place in the valence band, and if there are fewer spin-up than spin-down holes available the XMCD spectrum will show a net negative $2p_{3/2}$ and positive $2p_{1/2}$ peak. However, such a picture does not explain why, e.g., in high-resolution Fe spectra the $2p_{3/2}$ peak is asymmetric and displays a positive tail at the high-energy side [8]. This tail is absent from the $2p_{1/2}$ peak, whereas from an itinerant model one might naively expect a similar line shape as in the $2p_{3/2}$ peak. Measurements, such as on ferromagnetic Mn, Cr and V thin layers, show that with reduced d count the line shape becomes even more asymmetric [5]. Although the additional information lying dormant in the spectra would be very useful—if only to verify the sum rule results—to date no systematic analysis has been established to reveal the origin of the spectral variations.

† e-mail address: g.vanderlaan@dl.ac.uk

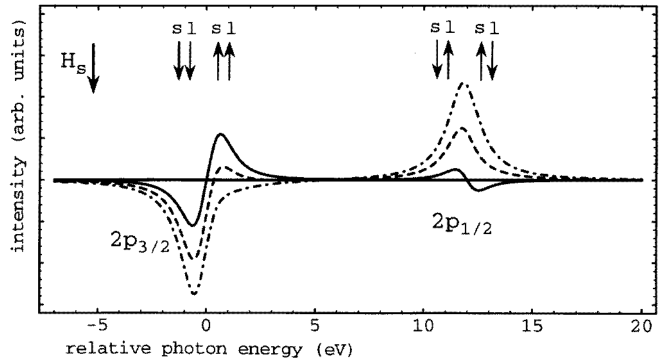

Figure 1. A schematic picture showing the origin of the line shape changes. The large 2p spin–orbit interaction together with a small exchange field H_s from the 3d electrons give coupled states, such as indicated at the upper- and lower-energy sides of each j level. This results in strongly different 2p XMCD spectra for a valence band with no spin polarization (full line), 50% spin polarization (dashed line), and complete spin polarization (dash–dotted line). Ground-state moments other than the spin moment have been taken equal to zero.

In this letter we will present a simple model to explain the 2p line shape variations. We show that by studying the influence of the ground-state moments it is possible to account for the aforementioned effects. The essence of the model is shown in figure 1. Apart from the strong core hole spin–orbit interaction which couples the spin and the orbit parallel or antiparallel in the two j levels, we consider a small exchange interaction which couples the spin of the core hole either net parallel or antiparallel to that of the valence electrons. In the presence of an applied magnetic field H_s, spin-up states will be at a higher photon energy than spin-down states. Figure 1 shows the coupling for the states at the upper- and lower-energy sides of each j level. In the absence of an orbital moment in the valence band, the XMCD signal is proportional to the expectation value of the core hole orbital moment [9]. When a core electron is excited into a level with no spin polarization we expect, similar to the case of photoemission, a dichroic signal with the same sign as the orbital moment of the created core hole. This spectrum is shown in figure 1 by the full line. On the other hand, when only spin-down holes are accessible in the valence band we will, due to spin conservation, observe a spectrum as given by the dash–dotted line. The dotted spectrum gives the intermediate situation with a spin polarization of 0.5. It is noted that this model is qualitatively correct for localized materials with core–valence exchange interaction as well as for itinerant materials with an effective spin field on the core levels. In ionic and covalent compounds the detailed line shape has been successfully explained in terms of multiplet and satellite structure [10], so we will restrict ourselves here to itinerant ferromagnets. The core spectra of these materials can be described, to first order, by an independent-particle model, possible refined by electron-correlation effects [9, 11]. We will show how to obtain *quantitative* information about the net 3d spin polarization from such a model, and we will also quantify the influence of the other ground-state moments on the spectrum.

The ground state of a material can be characterized by the multipole moments $\langle w^{xyz} \rangle$, where the orbital moment x and the spin moment y are coupled to a total moment z [12]. This notation will allow a systematic classification, which is well worth the initial confusion of the unfamiliar reader. Moments with even x describe the shape of the charge distribution and moments with odd x describe an orbital motion. An underscore signifies that the moment is taken not over the electrons but over the *holes*, which is required for x-ray absorption. Thus $\langle \underline{w}^{000} \rangle = n_h$ gives the number of holes. Further, the 3d shell contains the spin–orbit coupling $\langle \underline{w}^{110} \rangle = -\sum_i l_i \cdot s_i$, the orbital magnetic moment $\langle \underline{w}^{101} \rangle = L_z/2$, the spin magnetic moment $\langle \underline{w}^{011} \rangle = 2S_z$, the 'magnetic dipole' term $\langle \underline{w}^{211} \rangle = 7T_z/2$ and the quadrupole moment $\langle \underline{w}^{202} \rangle = -Q_{zz}/2$. An advantage of the advocated w-tensors is the normalization, i.e. $\langle \underline{w}^{xyz} \rangle = (-)^z$ for a ground state with a single hole, i.e. d^9.

We recall that for an electron from a core level c, $\frac{1}{2}$, j with orbital, spin and angular components γ, σ, m the transition probability into an incompletely filled valence shell l with orbital components λ using q-polarized electric dipole radiation along the magnetization direction is given by an operator [2, 13]

$$T_q = \sum_{\gamma\sigma} (-)^{l+j-\lambda-m} \begin{pmatrix} l & 1 & c \\ -\lambda & q & \gamma \end{pmatrix} \begin{pmatrix} j & \frac{1}{2} & c \\ -m & \sigma & \gamma \end{pmatrix} l^\dagger_{\lambda\sigma} j_{m\sigma} \tag{1}$$

where $l^\dagger_{\lambda\sigma}$ is a creation operator, $j_{m\sigma}$ is an annihilation operator, and the factors represented by the parenthesis are $3jm$ coefficients. Reduced-matrix elements leading only to an overall scaling have been omitted. This gives the x-ray absorption spectrum with q-polarized light of frequency ω for a ground state $|g\rangle$ and final states $|f\rangle$ as

$$I_q(\omega) = \langle g|T_q^\dagger|f\rangle\langle f|T_q|g\rangle \delta\big(E_f - \omega - E_g\big) \tag{2}$$

and the XMCD signal is $I = I_1 - I_{-1}$.

It is straightforward to express the dichroic signal of the jm final states as a linear combination of ground-state moments [14]

$$I_{jm} = \sum_{xyz} \langle \underline{w}^{xyz} \rangle C^{xyz}_{jm} \tag{3}$$

where the coefficients C^{xyz}_{jm} give the probability to create a core hole with quantum numbers jm for a ground state moment $\langle \underline{w}^{xyz} \rangle$ equal to unity.

To expand the signal of a j level in multipole moments r we write

$$C^{xyz}_{jm} = \sum_r C^{xyzr}_j u^r_{jm} \tag{4}$$

where the m-dependence is contained in

$$u^r_{jm} \equiv (2r+1)(-)^{j-m} n_{jr} \begin{pmatrix} j & r & j \\ -m & 0 & m \end{pmatrix} \tag{5}$$

where $n_{jr} \equiv \begin{pmatrix} j & r & j \\ -j & 0 & j \end{pmatrix}$. This normalization has been chosen such that $\sum_m u^r_{jm} = \delta_{r0}$ and $\sum_{r=0,2j} u^r_{jj} = 1$. Substitution of (4) into (3) gives

$$I_{jm} = \sum_{xyz} \langle \underline{w}^{xyz} \rangle \sum_r C^{xyzr}_j u^r_{jm} \tag{6}$$

so the coefficients C^{xyzr}_j give the probability of creating a core hole with multipole moment r in the j level for unit ground state moments $\langle \underline{w}^{xyz} \rangle$. Substitution of (5) and (6) into the definition of the rth moment of the j level, $I^{(r)}_j$, allows us to write the latter as a function of ground-state moments,

$$I^{(r)}_j \equiv n^{-1}_{jr} \sum_m I_{jm} (-)^{j-m} \begin{pmatrix} j & r & j \\ -m & 0 & m \end{pmatrix} = \sum_{xyz} \langle \underline{w}^{xyz} \rangle C^{xyzr}_j. \tag{7}$$

The intensities of the jm sublevels can be calculated from (1) and (2). The resulting coefficients C^{xyz}_{jm} for each d-shell moment $\langle \underline{w}^{xyz} \rangle$ in the $p \to d$ XMCD is given in table 1, together with the expressions for $\sum_r C_j^{xyzr} u_{jm}^r$ obtained using (4) and (5). From table 1 it is clear that ground moments with even (odd) z induce only odd (even) moments r. The sum rules are also immediately obvious. Since summation over m gives $u_j^0 = 1$ and $u_j^{r\neq 0} = 0$, the signal integrated over both edges is $I_{3/2}^{(0)} + I_{1/2}^{(0)} = 3\langle \underline{w}^{101}\rangle$ and the weighted difference is $I_{3/2}^{(0)} - 2I_{1/2}^{(0)} = \langle \underline{w}^{011}\rangle + 2\langle \underline{w}^{211}\rangle$.

Table 1. Coefficients C_{jm}^{xyz} of the jm sublevels and resulting expressions $\sum_r C_j^{xyzr} u_{jm}^r$ of the j levels for *unit* ground-state moments $\langle \underline{w}^{xyz}\rangle$ in the p $\rightarrow$ d magnetic circular dichroism. The w-tensors are also expressed in traditional notation.

		$\underline{w}^{000}$	$\underline{w}^{110}$	$\underline{w}^{101}$	$\underline{w}^{011}$	$\underline{w}^{211}$	$\underline{w}^{202}$
$j\ m$	n_h	$-l\cdot s$	$L_z/2$	$2S_z$	$7T_z/2$	$-Q_{zz}/2$	
$\frac{3}{2}, -\frac{3}{2}$	$-\frac{1}{4}$	$-\frac{1}{5}$	$\frac{3}{5}$	$\frac{1}{4}$	$\frac{1}{5}$	$-\frac{1}{2}$	
$\frac{3}{2}, -\frac{1}{2}$	$-\frac{1}{12}$	$-\frac{1}{15}$	$\frac{2}{5}$	$-\frac{1}{12}$	$\frac{2}{15}$	$-\frac{1}{6}$	
$\frac{3}{2}, +\frac{1}{2}$	$\frac{1}{12}$	$\frac{1}{15}$	$\frac{2}{5}$	$-\frac{1}{12}$	$\frac{2}{15}$	$\frac{1}{6}$	
$\frac{3}{2}, +\frac{3}{2}$	$\frac{1}{4}$	$\frac{1}{5}$	$\frac{3}{5}$	$\frac{1}{4}$	$\frac{1}{5}$	$\frac{1}{2}$	
$\frac{1}{2}, +\frac{1}{2}$	$\frac{1}{6}$	$-\frac{1}{6}$	$\frac{1}{2}$	$-\frac{1}{6}$	$-\frac{1}{3}$	$\frac{1}{3}$	
$\frac{1}{2}, -\frac{1}{2}$	$-\frac{1}{6}$	$\frac{1}{6}$	$\frac{1}{2}$	$-\frac{1}{6}$	$-\frac{1}{3}$	$-\frac{1}{3}$	
$\frac{3}{2}$	$\frac{5}{9}u^1$	$\frac{4}{9}u^1$	$2u^0 + \frac{2}{5}u^2$	$\frac{1}{3}u^0 + \frac{2}{3}u^2$	$\frac{2}{3}u^0 + \frac{2}{15}u^2$	$\frac{10}{9}u^1$	
$\frac{1}{2}$	$\frac{1}{3}u^1$	$-\frac{1}{3}u^1$	u^0	$-\frac{1}{3}u^0$	$-\frac{2}{3}u^0$	$\frac{2}{3}u^1$	

For the line shape of the spectra we need to know both the intensity distribution and the energy distribution over the jm levels. If we assume an independent-particle model [9, 11], each j level is split by an effective exchange field H_s into $2j+1$ sublevels with energy positions

$$E_{jm} = H_s m \frac{j(j+1) + s(s+1) - l(l+1)}{2j(j+1)}. \tag{8}$$

Since the spectral distribution is $I_{jm}(\omega) = I_{jm}\delta(E_{jm} - \omega - E_g)$ with a constant energy spacing $H_s/3$ of the sublevels in both j levels, the conversion from multipole moments to spectral moments is easy. The main thing to watch is that the energy sequence of the m sublevels in the $j = \frac{1}{2}$ is reversed compared to that in the $j = \frac{3}{2}$ level, so that odd moments of the $j = \frac{1}{2}$ level reverse in sign. The separate contributions to the spectra can be obtained directly from table 1 and are shown in figure 2 normalized per unit $(-)^z\langle \underline{w}^{xyz}\rangle$. Operators with odd z give a symmetric signal for each j level, whereas operators with even z give an antisymmetric signal. The moments with $z = 1$ are of special interest because they match the moment transferred by the photon in circular dichroism. As expected from the sum rules the operator $\underline{w}^{101}$ gives a statistical distribution over the j levels ($\propto 2j+1$). The operators $\underline{w}^{011}$ and $\underline{w}^{211}$ will not change the total intensity but transfer intensity between the two j levels. From figure 2 it can be checked that the $j = \frac{1}{2}$ signal disappears when $\langle \underline{w}^{101}\rangle = \langle \underline{w}^{011}\rangle = \langle \underline{w}^{211}\rangle$. This is in agreement with the jj coupled sum rule [15], which states that the $p_{1/2}$ signal is proportional to the j_z component of the ground-state $d_{3/2}$ level, which is zero under the given conditions. Operators with $z \neq 1$ can only shift the intensity *within* a j level. All moments give a negative signal at the low-energy side of the $j = \frac{3}{2}$ peak.

When the values of the d-shell moments are known, the 2p spectrum can be obtained from (3) by simply adding up all the contributions with their relative weights. In figure 2 it

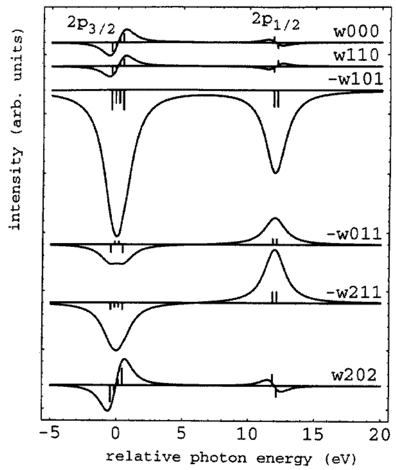

Figure 2. Separate contributions to the 2p XMCD for the 3d ground-state moments $(-)^z\langle \underline{w}^{xyz}\rangle$. Each signal is given for a moment equal to one. Core spin–orbit parameter $\zeta(2p) = 8$ eV, exchange field $H_s = 0.9$ eV. The signals of the jm levels, given by the sticks, have been convoluted with a Lorentzian of $\Gamma = 0.9$ eV.

is seen that, if all moments had the same value, the shape of the spectrum would be strongly dominated by the orbital moment $\langle \underline{w}^{101}\rangle$. However, in a solid the orbital moment is usually quenched, so other moments will become important. In itinerant 3d magnets $\langle \underline{w}^{110}\rangle$ and $\langle \underline{w}^{101}\rangle$ are often an order of magnitude smaller than $\langle \underline{w}^{000}\rangle$ and $\langle \underline{w}^{011}\rangle$. The moments $\langle \underline{w}^{211}\rangle$ and $\langle \underline{w}^{202}\rangle$ vanish in cubic systems, but can become relatively important at the surface where the symmetry is broken. Therefore, the shape of the dichroism spectrum is primarily determined only by the 3d spin polarization $P_s \equiv (n_\uparrow - n_\downarrow)/(n_\uparrow + n_\downarrow) = -\langle \underline{w}^{011}\rangle/\langle \underline{w}^{000}\rangle$. For $P_s = 0$ the spectrum is equal to that of $\langle \underline{w}^{000}\rangle$, which is given in figure 2 and which exhibits completely antisymmetric peaks. An additional contribution from $\langle \underline{w}^{011}\rangle$ will result in more symmetric peaks. If we neglect the other moments the relative peak asymmetry, $I_j^{(1)}/I_j^{(0)}$, as obtained from table 1, is equal to $-5/(3P_s)$ and $-1/P_s$ for the $j = \frac{3}{2}$ and $\frac{1}{2}$ levels, respectively. Thus the peak asymmetry is inversely proportional to the spin polarization with a larger coefficient for the $j = \frac{3}{2}$ level in agreement with experimental results [5–8]. Hard ferromagnets, such as nickel with an almost completely filled majority spin band, will display very symmetric peaks, while soft ferromagnetics, such as ultra-thin overlayers of Mn and Cr, display dispersive-like structures. However, the other moments also play a role, albeit less pronounced. As a realistic example we show in figure 3 the calculated spectra for a ground state with *per hole* $\langle \underline{w}^{110}\rangle = 0.15$, $\langle \underline{w}^{101}\rangle = -0.03$, $\langle \underline{w}^{211}\rangle = -0.01$, and $\langle \underline{w}^{202}\rangle = 0.01$ for different values of P_s. The results confirm clearly the intuitive picture given in figure 1. The difference between the curves in figure 1 and those in figure 3 for $P_s = 0$, 0.5, and 1 is due to the influence of the spin–orbit coupling and the orbital magnetic moment.

As mentioned in the introduction, to a first approximation, the exchange interaction in an atomic model acts in a similar manner to the exchange field in a one-particle model. However, a strong core hole interaction due to localization of the d states can induce satellite structure, as in the case of nickel [16], or multiplet structure, as in Mn [5]. The above model is then no longer adequate and one has to take the core hole interaction implicitly into account [10].

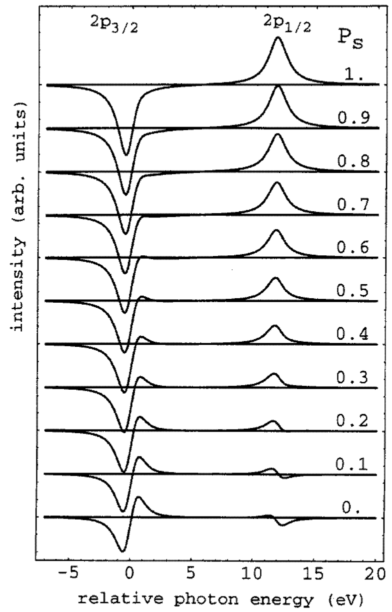

Figure 3. The 2p XMCD for different 3d spin polarizations $P_s = -\langle \underline{w}^{011} \rangle / \langle \underline{w}^{000} \rangle$ and a spin–orbit interaction $\langle \underline{w}^{110} \rangle = 0.15$, orbital moment $\langle \underline{w}^{101} \rangle = -0.03$, magnetic dipole term $\langle \underline{w}^{211} \rangle = -0.01$, and quadrupole moment $\langle \underline{w}^{202} \rangle = 0.01$ *per hole*. $\zeta(2p) = 8$ eV, $H_s = 0.9$ eV, and Lorentzian line broadening $\Gamma = 0.9$ eV.

Summarizing, we have shown that the line shape of the x-ray magnetic dichroism spectrum is primarily determined by the net spin polarization in the valence band, with other ground-state moments playing a less prominent role. In a given spectrum we can easily separate the ground-state moments with even z from those with odd z, because they induce odd and even spectral moments, respectively. Sometimes it will even be possible to separate the individual ground-state moments, because of their different relative contributions at each jm sublevel. In a carefully designed experiment, e.g. on epitaxially grown thin films of different thicknesses, it might even be possible to separate the magnetic dipole term from the spin magnetic moment. Finally, the described model provides insight into the influence of the ground-state properties on the spectrum. This will also greatly simplify any calculational fit of the spectrum since it removes the need for a large number of calculations trying different parameter sets.

References

[1] Thole B T, Carra P, Sette F and van der Laan G 1992 *Phys. Rev. Lett.* **68** 1943
[2] Carra P, Thole B T, Altarelli M and Wang X 1993 *Phys. Rev. Lett.* **69** 2307
[3] Luo J, Trammell G T and Hannon J P 1995 *Phys. Rev. Lett.* **71** 287
[4] Wu R, Wang D and Freeman A J 1994 *J. Magn. Magn. Mater.* **132** 103
[5] O'Brien W L, Tonner B P, Harp G R and Parkin S S P 1994 *J. Appl. Phys.* **76** 6462
[6] Chen C T *et al* 1995 *Phys. Rev. Lett.* **75** 152
Boske T *et al* 1995 *Appl. Phys.* A **61** 119
Harp G R *et al* 1995 *Phys. Rev.* B **51** 3293
Tischer M *et al* 1996 *Phys. Rev. Lett.* **76** 1403

[7] Lovesey S W and Collins S P 1996 *X-Ray Scattering and Absorption by Magnetic Materials* (Oxford: Clarendon)
[8] Dürr H A, Guo G Y, Thole B T and van der Laan G 1996 *J. Phys.: Condens. Matter* **8** L111
[9] van der Laan G 1995 *Phys. Rev.* B **51** 240
[10] van der Laan G and Thole B T 1991 *Phys. Rev.* B **43** 13 401. Note that the XMCD signal is here defined with opposite sign.
[11] Ebert H 1989 *J. Phys.: Condens. Matter* **1** 9111
[12] van der Laan G and Thole B T 1995 *J. Phys.: Condens. Matter* **7** 9947
[13] Varshalovich D A, Moskalev A N and Khersonskii V K 1988 *Quantum Theory of Angular Momentum* (Singapore: World Scientific)
[14] van der Laan G 1997 *Phys. Rev.* B **55** 8086
[15] van der Laan G and Thole B T 1996 *Phys. Rev.* B **53** 14 458, equation (38)
[16] van der Laan G and Thole B T 1992 *J. Phys.: Condens. Matter* **4** 4181